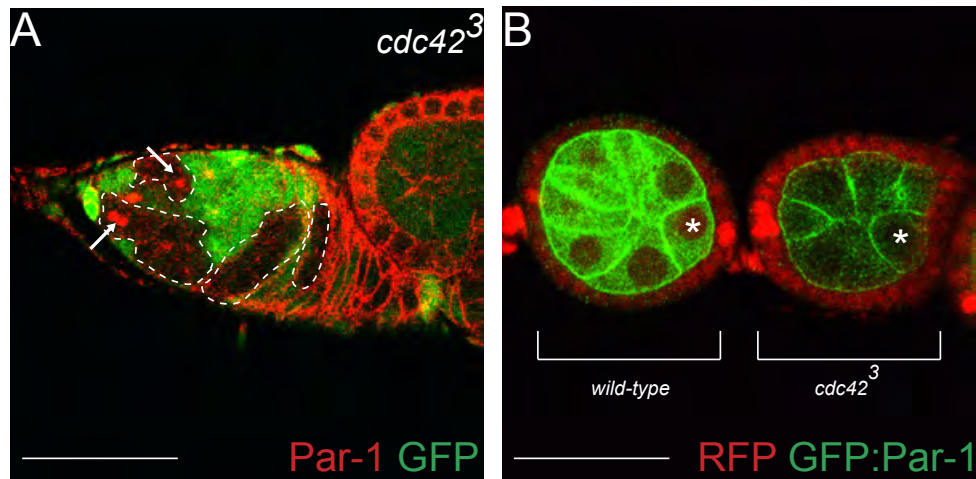
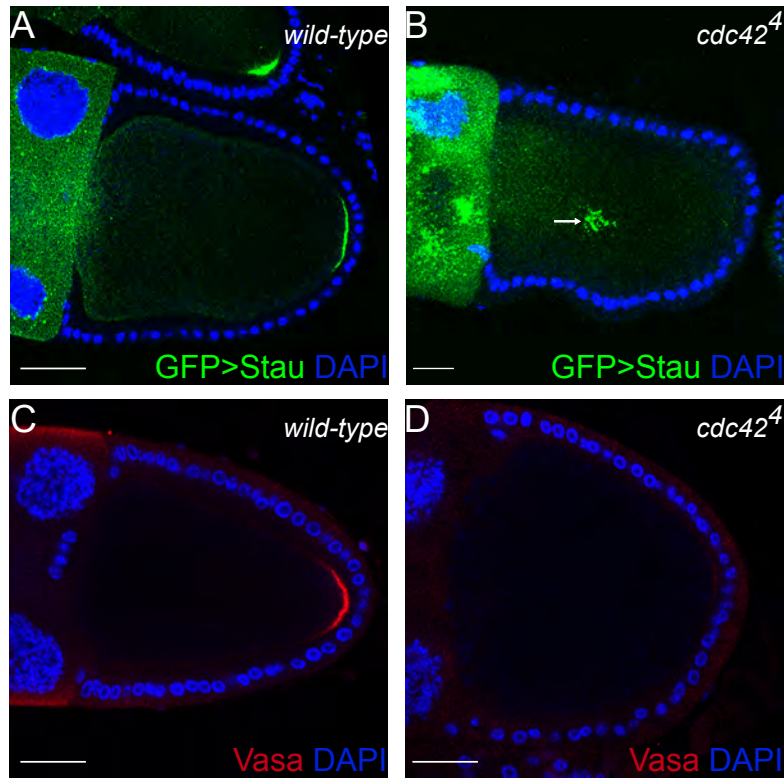


**Fig. S1. Nurse cell and oocyte development in *Cdc42<sup>3</sup>* and *Cdc42<sup>4</sup>* egg chambers.** (A) *Cdc42<sup>3</sup>* mutant egg chambers develop only until stage 5 and display 16 nurse cells. Several stacks are displayed to show all 15 nuclei and oocyte of wild-type egg chamber and the 16 nurse cells of the mutant egg chamber. (B) Some *Cdc42<sup>4</sup>* mutant egg chambers develop until stage 5 and display 16 nurse cells. Two stacks are displayed to show all 15 nuclei and oocyte of the wild-type egg chamber and the 16 nurse cells of the mutant egg chamber. Scale bars: 25  $\mu$ m.



**Fig. S2. Par-1 localization is mildly affected by loss of *Cdc42*.** (A,B) *Cdc42<sup>3</sup>* mutant clones are marked by loss of nuclear GFP (A) or RFP (B). Par-1 localizes normally to the fusome in mutant clones (A). Mutant clones are encircled with a dashed line. Arrows point to Par-1-positive fusome. GFP-Par-1 localization is weaker in *Cdc42<sup>3</sup>* germline clones as compared with control egg chambers (B; 20%,  $n=15$ ). Scale bars: 50  $\mu$ m.



**Fig. S3. Staufen and Vasa mislocalize in *Cdc42*<sup>4</sup> germline clones.** (A,B) *Cdc42*<sup>4</sup> mutant clones recovered using the dominant female sterile technique (ovoD) display mislocalized GFP-Staufen protein (green, 25% mislocalization, *n*=118) at stage 9/10 and a mispositioned oocyte nucleus (4% mispositioning, *n*=118). Arrow indicates nucleus and GFP-Staufen localization. (C,D) *Cdc42*<sup>4</sup> mutant clones recovered using the dominant female sterile technique (ovoD) display mislocalized Vasa (red, 30% mislocalization, *n*=56) at stage 10. Scale bars: 25  $\mu$ m.

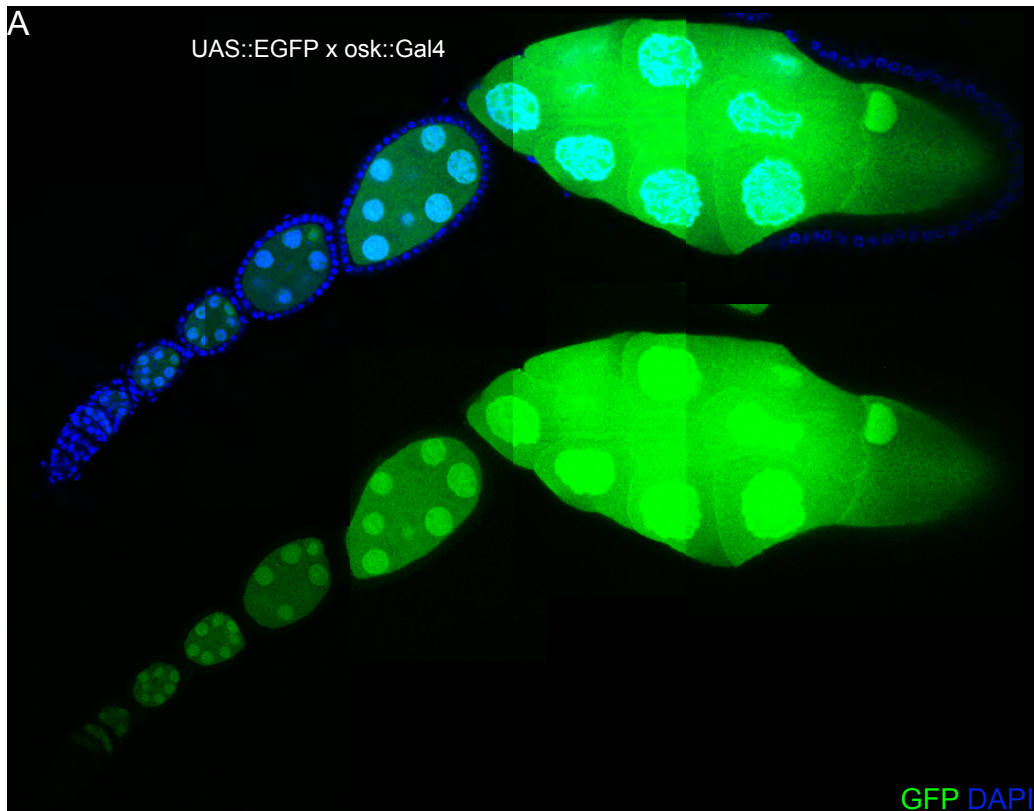


**Fig. S4. Activity of the germline driver *oskar*>*Gal4*.** Ovariole from flies expressing UAS>EGFP using the driver *oskar*>*Gal4*. *oskar*>*Gal4* drives expression from early to late oogenesis.

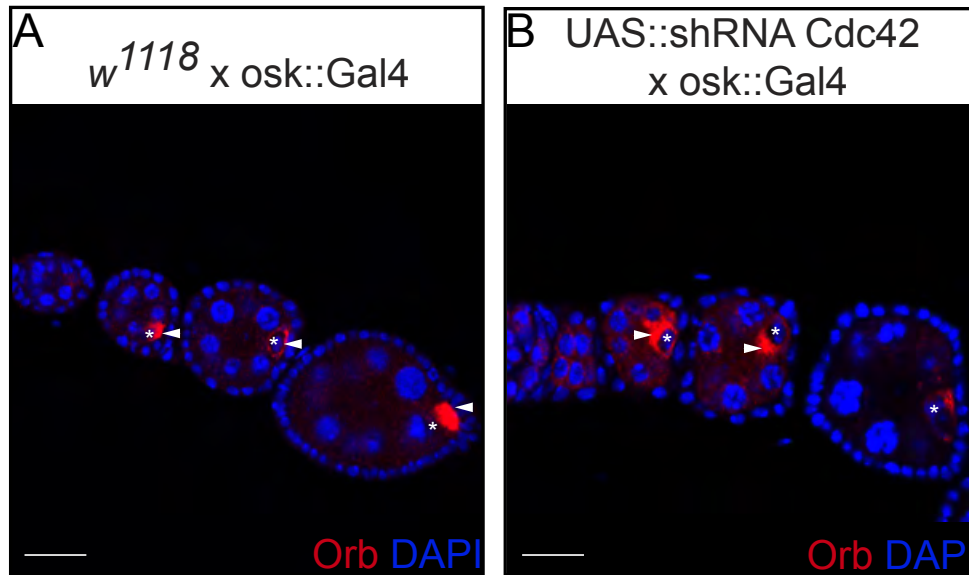


**Fig. S5. Knockdown of Cdc42 results in failure of Orb translocation.** Orb protein does not translocate from the anterior to the posterior of the oocyte upon knockdown of Cdc42 (26%,  $n=81$ ). (A) Control; (B) knockdown. Asterisks mark oocytes of interest; arrowheads pointing to the right mark anterior protein localization; arrowheads pointing to the left mark posterior protein localization. Scale bars: 25  $\mu\text{m}$ .

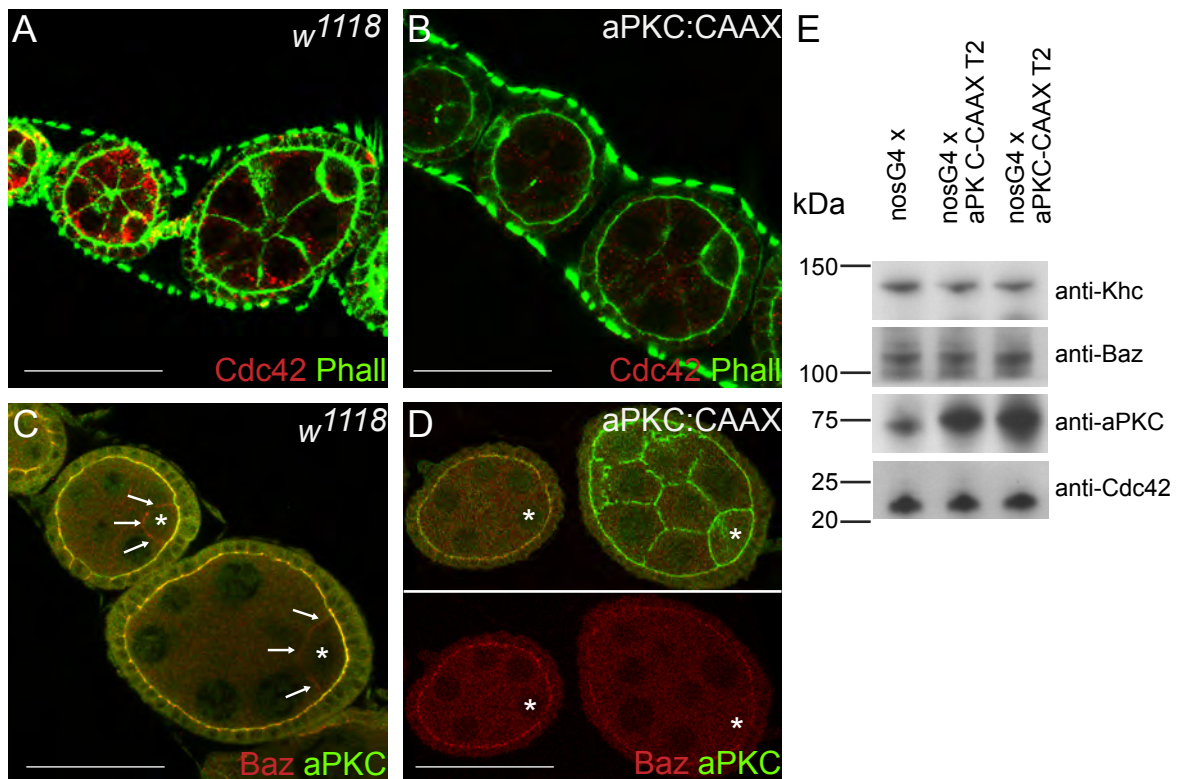


**Fig. S6. Overexpression of membrane-tethered aPKC reduces cortical localization of polarity proteins.** (A,B) Cdc42 (red) and actin (green) localization in  $w^{1118}$  flies (A) and flies expressing UASp>aPKC-CAAX driven by *nanos*>*Gal4* (B). (C,D) Baz (red) and aPKC (green) localization in  $w^{1118}$  flies (C) and flies expressing UASp>aPKC-CAAX driven by *nanos*>*Gal4* (D). Arrows point to specific protein localization. (E) Protein levels are not visibly reduced on western blot when membrane-tethered aPKC is expressed in the germline. Scale bars: 25  $\mu\text{m}$ .

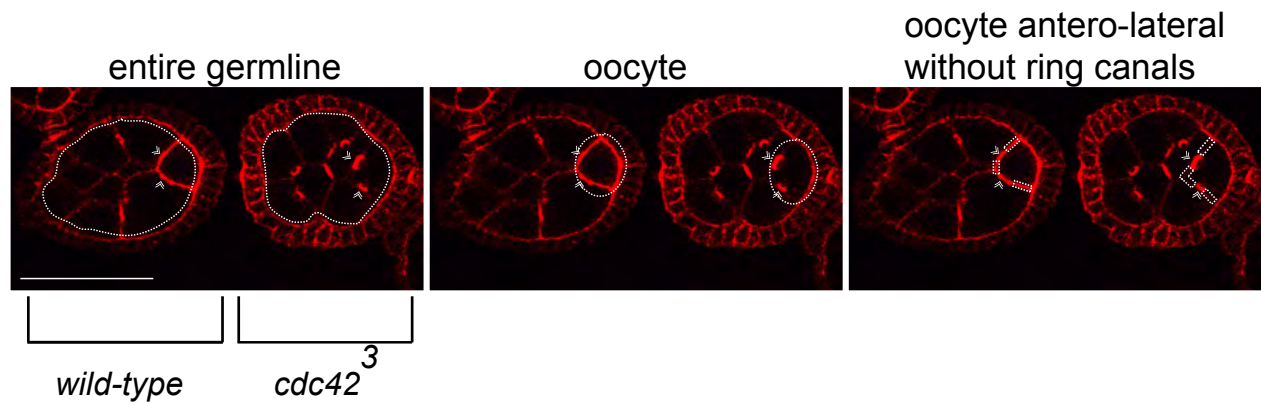


**Fig. S7. Analysis of actin levels in mutant and wild-type egg chambers.** Actin levels were quantified by measuring the mean intensity of Rhodamine-phalloidin in either the whole germline tissue of the cyst (left image) or the oocyte only (middle image). To consider only regions where Cdc42 localization is enriched, the anterior and lateral regions of oocytes were also analyzed (right image), not taking into account the ring canals (double arrowheads). Note that analysis was always performed on *Cdc42*<sup>3</sup> mutant egg chambers that could be directly compared with a younger wild-type egg chamber of the same ovariole.

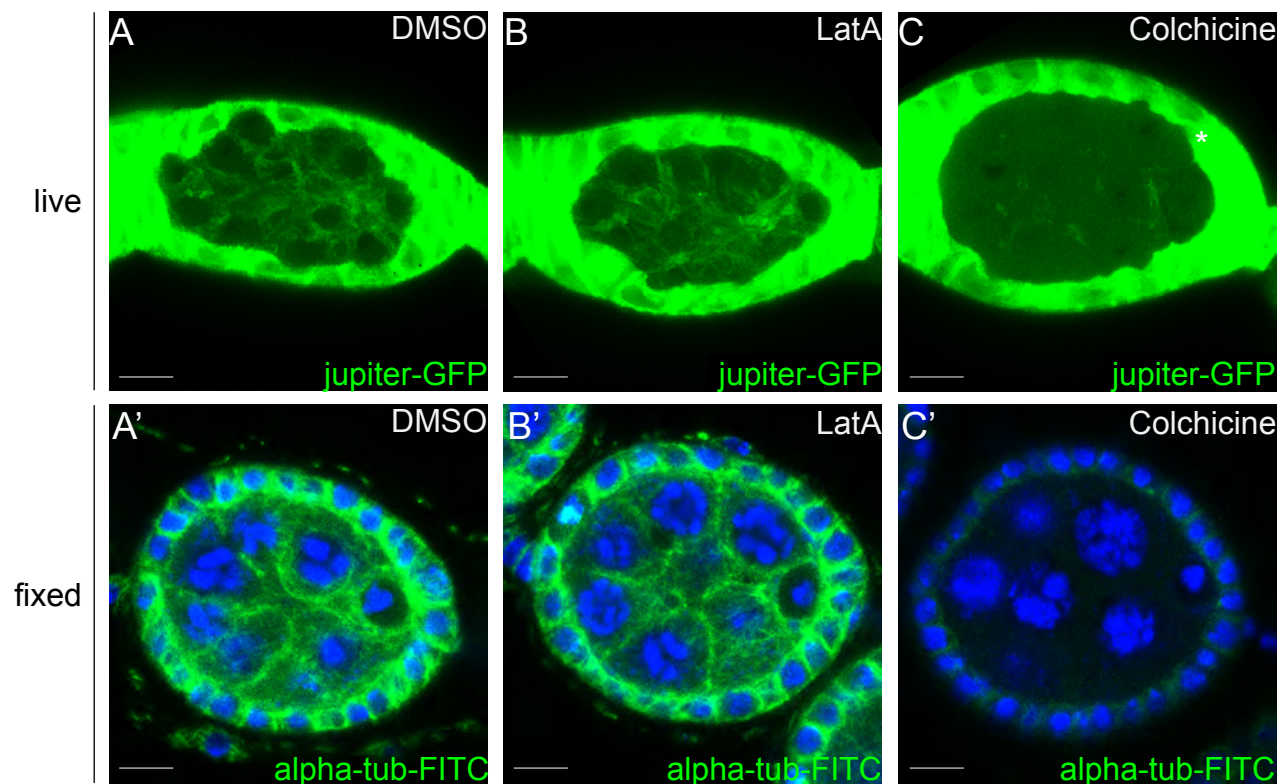


**Fig. S8. Latrunculin A treatment does not interfere with microtubules.** (A-C') Live imaging (A,B,C; Jupiter-GFP) and fixed imaging (A',B',C';  $\alpha$ -tubulin-FITC) of microtubules after drug treatment. Flies were fed with DMSO (1:10; A,A'), 1 mM Latrunculin A (B,B') or 50  $\mu$ g/ml Colchicine (C,C') for 16 hours prior to dissection. Live imaging was performed on Jupiter-GFP flies. Images show maximal projections of 160 images taken with an imaging rate of 1.95 seconds/image. For fixed analysis, *w*<sup>1118</sup> flies were used. Scale bars: 25  $\mu$ m.

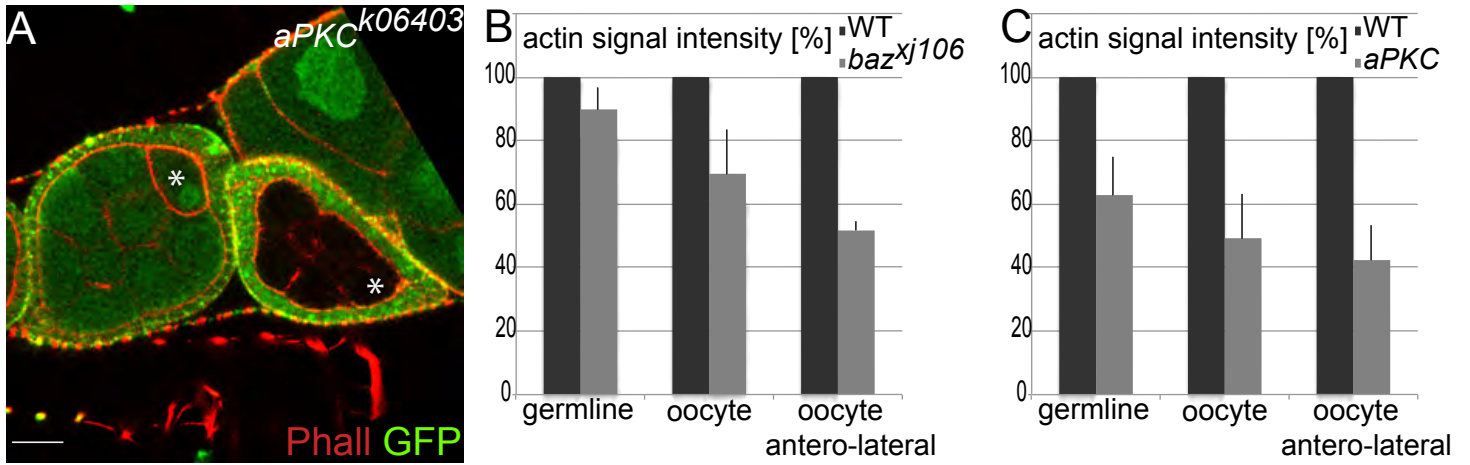


**Fig. S9. Cdc42 and Par proteins cooperate to organize the actin cytoskeleton and establish oocyte polarity.** (A) *aPKC<sup>K06403</sup>* mutant egg chambers marked by loss of nuclear GFP result in loss of the pronounced actin cytoskeleton at the anterolateral cortex of the oocyte (86%,  $n=7$ ). The actin cytoskeleton is labeled using fluorescently labeled phalloidin. Scale bar: 25  $\mu$ m. (B,C) Quantification of phalloidin staining in wild-type, *baz<sup>xj106</sup>* (B) and *aPKC<sup>K06403</sup>* (C) mutant egg chambers (left bars), oocytes (middle bars), and the anterior and lateral regions of oocytes (avoiding the posterior, which is in contact with the somatic cells; right bars). Standard error is indicated.

**Table S1. Experiments using drugs to specifically inhibit Rho, Rac or Cdc42 were inconclusive**

<b>Orb mislocalization</b>	<b>Drug treatment</b>			
	<b>DMSO</b>	<b>Rac1 inhibitor</b>	<b>H-1152</b>	<b>IPA-3</b>
Mislocalized at anterior	1	5	6	11
Normal	65	30	30	58
Absent	0	1	0	0
Total	66	36	36	69
<b>Orb mislocalization (%)</b>	<b>1.5</b>	<b>17</b>	<b>17</b>	<b>16</b>
Notes				Morphology affected

Inhibition of Rac GTPase with 50  $\mu$ M Rac inhibitor, inhibition of Rho GTPase with 2  $\mu$ M H-1152 and inhibition of Cdc42-mediated events with 100  $\mu$ M IPA-3 treatment for 4 hours did not lead to conclusive results because the morphology of the ovarioles was affected.